Research Article

Florian Loosen*, Norbert Lindlein and Klaus Donner

Telecentric line scanning system based on a ring surface mirror for inline processes

DOI 10.1515/aot-2016-0010
Received February 4, 2016; accepted April 7, 2016; previously published online May 9, 2016

Abstract: In many industrial applications, an inline measurement of a production process poses a difficult challenge for any optical system. Therefore, telecentric optical systems are being used to ensure an independence of the magnification of the object from the working distance. Usually, telecentric optical systems are impractical for inline applications with large objects due to the size of the telecentric optical system, which has to be larger than the object. Therefore, a new approach of telecentric line scanning systems was developed to gain access to this advantage.

Keywords: industrial applications; inline processes; measuring system; optical design and simulation; ring surface mirror; telecentric system.

OCIS code: 080.0080; 080.3620; 080.4035; 080.6755; 110.0110; 110.2970; 120.0120; 120.5800.

1 Introduction

In inline processing [1], e.g. for scratch detection of aluminum rolled sheets or the detection of the dimensions of printed parts on polymer sheets (Figure 1), telecentric systems [2, 3] are used to measure these contours. The company alfavision GmbH had the idea to create a so-called 3D telecentric scanner [4], using a torus mirror as the main optical component and a line camera in order to have a relatively cheap detector with high lateral resolution. To fabricate a low cost and highly practicable system, providing high resolutions in axial and lateral directions, many design rules have to be considered. This article is intended to describe the basic principle of this telecentric line scanning system, whose design is a new approach to combine the advantages of a telecentric lens system with a compact system setup [5].

2 System setup

Figure 2 shows the schematic view of the system, consisting of two subsystems (the torus mirror and the imaging system). Furthermore, important parts are the illumination and the detection.

High-power LEDs provide the illumination of the object, incident under a small angle to the surface normal. In addition, a scattering plate in front of the LEDs is used for homogenization. The illumination path of the system is shaped as an arc of a circle. The detection is done by a line scan camera, positioned in the plane of the real image of the illuminated area on the object surface. The imaging system in Figure 2 is drawn as a 'black box' (yellow cylinder), described in chapter 4. Two image planes are shown (dashed and continuous red lines). One virtual intermediate image plane (curved) generated by the torus mirror and one real image plane (flat) generated by the imaging system (subsystem of the telecentric scanner).

3 Mirror design

A new method to fulfill the telecentric condition of the system concept is to use a torus mirror. Through the rotationally symmetrical geometry of the mirror, all chief rays pass the center of the rotation axis in horizontal direction. By using a special geometry at the vertical direction, a 90° deflection is generated. The optical path has to fulfill the

***Corresponding author: Florian Loosen,** Institute of Optics, Information and Photonics, Friedrich-Alexander-Universität Erlangen-Nürnberg (FAU), Staudtstraße 7/B2, 91058 Erlangen, Germany, e-mail: florian.loosen@fau.de
Norbert Lindlein: Institute of Optics, Information and Photonics, Friedrich-Alexander-Universität Erlangen-Nürnberg (FAU), Staudtstraße 7/B2, 91058 Erlangen, Germany
Klaus Donner: alfavision GmbH & Co. KG, Freyunger Straße 4, 94116 Hutthurm, Germany

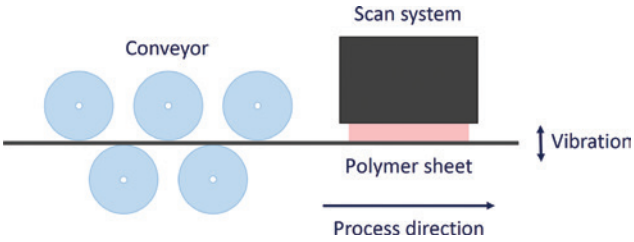

Figure 1: Principle sketch of an inline process (contour detection of printed polymer sheets).

paraxial image equation (1) [6], where g, b, and f represent object and image distance as well as the focal length of the mirror, respectively.

$$\frac{1}{b}-\frac{1}{g}=\frac{1}{f}\rightarrow b=\frac{fg}{g+f} \tag{1}$$

For the cross section of the mirror (the 'special geometry at the vertical direction'), the four different conic section designs (circle, ellipse, parabola, hyperbola) were analyzed. The best imaging performance is generated by a hyperbolic conic section (Figure 3). This creates an image in the plane of the conic section, which is free of aberrations. This is not true for the other three possible geometries, wherefore the following discussion is limited to the hyperbola. The main form of the hyperbola equation (2) [7] yields the geometry of the conic section.

$$x^2+(y+g)^2=(\sqrt{(x-b)^2+y^2}-r)^2 \tag{2}$$

Here, x and y describe the local coordinate system, g and b (object and image distance) the shift of the corresponding axis intercept, and r the radius.

Through reflection on the conic section, rays arising from an object point (which is identical to a focal point) form a virtual image point coinciding with the other focal point of the hyperbola.

4 Imaging system design

Owing to the rotationally symmetrical mirror, a curved intermediate image of the scan line occurs, which has to be imaged on a plane detector surface (see Figures 2 and 4). Therefore, the imaging system (Triplet or Planar) has to fulfill the Petzval condition [8] given by the Petzval equation (3).

$$\frac{1}{r_p}=\sum_i \frac{1}{r_i}\left(\frac{1}{n_{i-1}}-\frac{1}{n_i}\right) \tag{3}$$

Here, r_p describes the radius of the Petzval surface (Petzval curvature of the image plane in the common case), r_i the radii of the different surfaces of the imaging system, labeled by the index i, as well as n_{i-1} and n_i the refractive indices of the homogeneous materials before and after surface i, respectively.

For all design and optimization steps, raytracing techniques were used to minimize the aberrations to get the best results for the whole setup. Two different approaches to the imaging system were examined and optimized by simulations. In both cases, the entrance pupil (aperture stop) of the imaging system coincides with the telecentricity stop of the entire system (axis of symmetry of the torus mirror).

First, a Triplet lens system [9] was designed. This low-cost setup of three lenses poses an easy way to

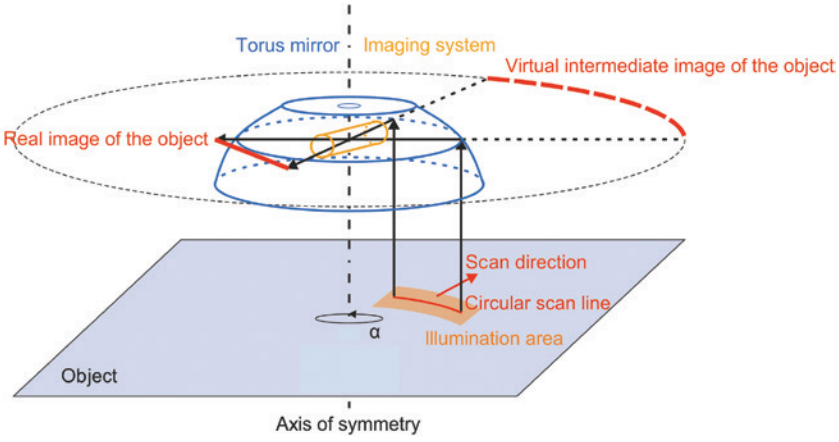

Figure 2: Schematic view of the telecentric scanning system with torus mirror, imaging system, and detector plane, which is lying on the position of the real image of the object. Object transformation from a circular scan curve in the object plane to a virtual intermediate image with subsequent imaging to a real image of the object.

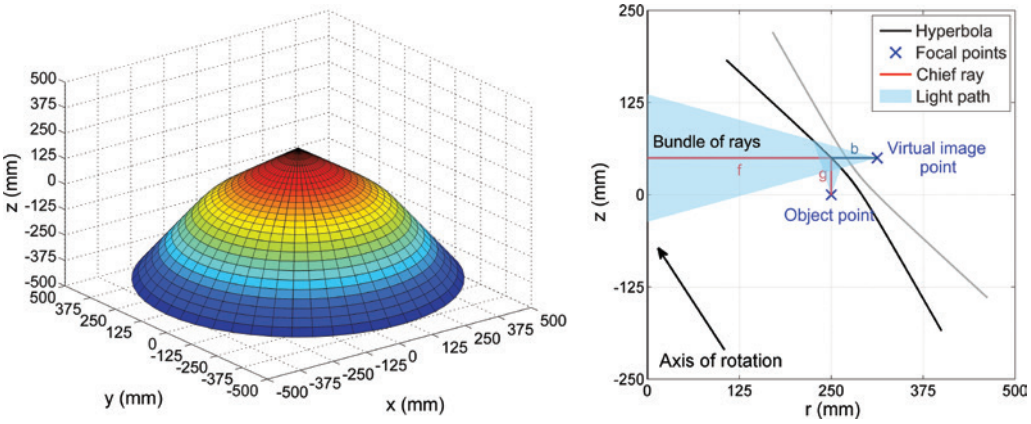

Figure 3: Rotation body (left) and section plane (right) of the rotation hyperbola. The negative branch of the hyperbola rotates around the z-axis (axis of rotation). This forms a torso, which is used as a torus mirror. The chief rays are deflected at the mirror under an angle of 90°. g, b, and f represent the object and image distance as well as the focal length of the mirror, respectively. The color-marked area describes the light path of all rays reflected at the negative branch.

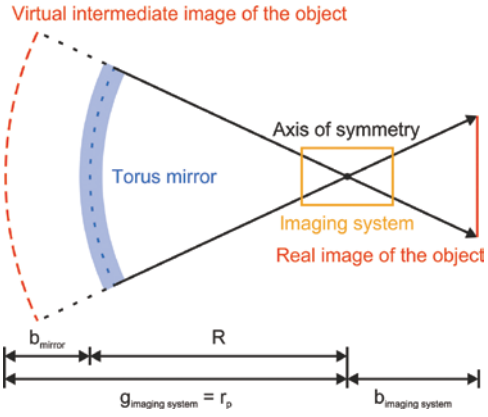

Figure 4: Sketch of the top view of the simulated telecentric scanning system with torus mirror, imaging system, and detector plane. The circular scan line itself with the object points is below the drawing plane. The entrance pupil of the imaging system coincides with the telecentricity stop. The object distance of the imaging system is approximately the radius of the Petzval sum.

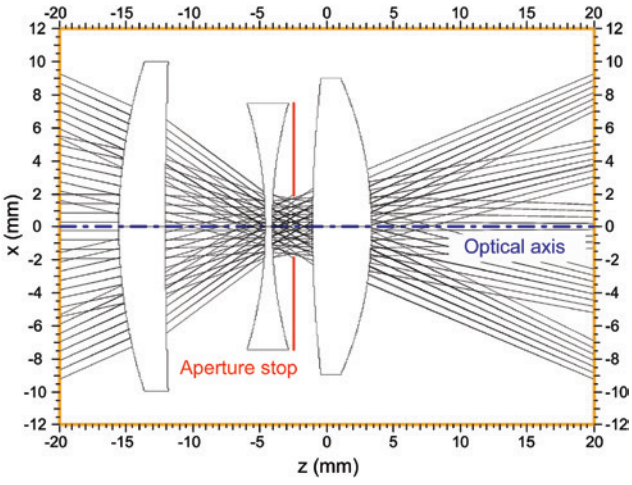

Figure 5: Top view of the designed imaging system (Triplet). The yellow frame symbolizes the black box drawn in Figures 2 and 4.

simultaneously optimize the imaging quality as well as minimize the optical aberrations of the system. The top view of the designed Triplet is shown in Figure 5, being composed of a meniscus, a biconcave lens, and a biconvex lens. The aperture stop is located between the biconcave and the biconvex lens.

The second design is a lens system based on a Planar [10]. The denotation 'Planar' is being used for concise distinction. The original design by Paul Rudolph consists of two menisci and two achromatic lenses, symmetrically arranged around the aperture stop of the imaging system, which was developed to reduce many wave aberrations (especially astigmatism and field curvature). Our design is non-symmetrical (the aperture stop is not centered symmetrically between the two inner lenses) and consists of a meniscus, two achromatic lenses with meniscal shape, and a biconvex lens (Figure 6).

5 Simulations

Two different simulation scenarios were performed, examining the performances of the imaging system alone as well as the entire scanning system. The results of the two scenarios are being presented both for Triplet and Planar approaches in comparison, with an object sided numerical aperture (NA_{obj}) of 0.009 and an illumination wavelength (λ) of 620 nm.

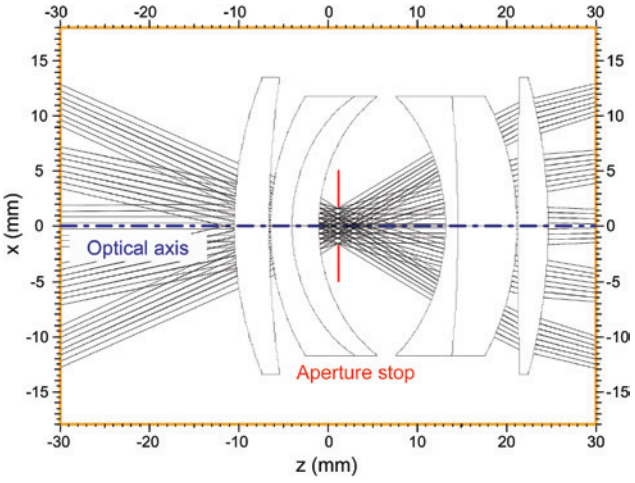

Figure 6: Top view of the designed imaging system (Planar). The yellow frame symbolizes the black box drawn in Figures 2 and 4.

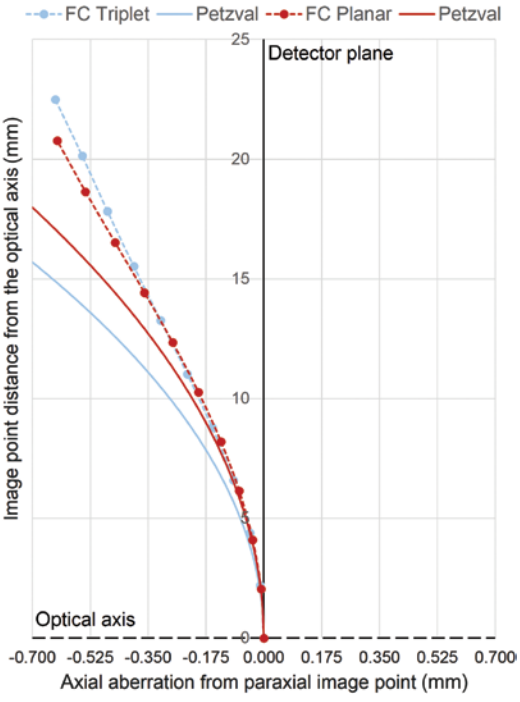

Figure 7: Field curvature of both imaging systems (Triplet and Planar) for a plane object plane. The dashed lines represent the simulated field curvature from different object angles (marked by points) and the solid lines the Petzval field curvature.

Considering the Petzval curvature (calculated using equation (3)) with the traced field curvature (FC) of both imaging systems (Triplet and Planar), the results for each imaging system are similar to each other (Figure 7). The difference between the Petzval curvature and simulated FC for larger field angles is due to the field aberrations for off-axis rays and the fact that the Petzval curvature describes the field curvature in both directions (meridional and sagittal plane). Here, only the meridional plane (the plane including the optical axis) is simulated, due to the line imaging of the system. The space between the detector plane and the simulated field curvature is approximately 650 µm (maximal deviation between detector plane and off-axis image points).

The consideration of both imaging systems (Triplet and Planar) for a curved object field produced the field curvature shown in Figure 8. Both designed lens systems provide good results. The maximal space between the detector plane and the field curvature of the image is approximately 50 µm, neglecting the last off-axis image point (especially for the Triplet design).

The wave aberrations (WAs) and the point spread function (PSF) of every image point (axial and off-axial) each show good results. The PV (peak-to-valley) value of the most distant off-axis image point is approximately 0.5 λ for the Triplet and 0.05 λ for the Planar design. The PSFs of those points in both cases are approximately 10 µm (equal to the detector pixel size).

The required lateral resolution [2] of the whole system at the object plane, given by equation (4), is 40 µm. With equations (1) and (4), all other system parameters can be calculated.

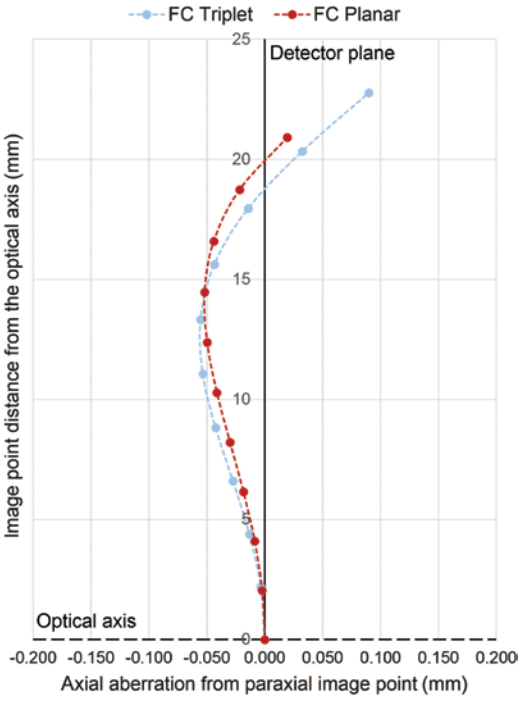

Figure 8: Field curvature of both imaging systems (Triplet and Planar) for a curved object plane. The dashed lines represent the simulated field curvature from different object angles (marked by points).

$$\Delta x \geq 0.61 \frac{\lambda}{NA_{obj}} \quad (4)$$

For example, these can be the axial resolution, the line widths (for known pixel size of the detector) in object and image plane, and the object and image sided distances. In equation (4), Δx represents the lateral resolution, λ the illumination wavelength, and NA_{obj} the object sided numerical aperture.

In addition to the curvature of the field, the image suffers from distortion, as using a simple lens design not all aberrations can be corrected for completely. Fortunately, this distortion can easily be corrected via image processing. In any case, image processing is necessary to backtrace from the transformed image points to the object points at the examined surface. The principle sketch of the reconstruction step of the image is shown in Figure 9. In (A), the curved scan line on the object surface is shown for equidistant scan points. (B) shows the transformed image (flat) on the line scan camera (red dots). The reconstructed image via image processing is shown in (C), with distortion correction.

Owing to the modular principle of the system, long lines can be generated. Therefore, several line scanners in alternate order can be merged together. The overlap of the scan lines can be corrected via image processing.

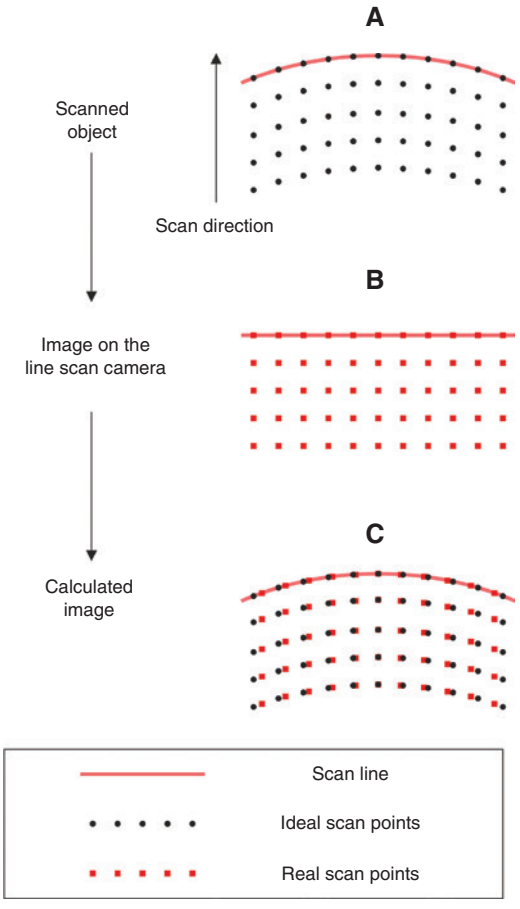

Figure 9: Principle sketch of the reconstruction of the image with backtracing from a plane to a curved image with distortion correction.

6 Redesign

For microscopic applications, an increased lateral resolution is necessary (desired lateral resolution at the object plane of 4 µm). Consequently, to increase the lateral resolution, a higher object sided numerical aperture is indispensable (NA_{obj} of 0.09). In addition, for a compact system, especially for microscopic applications, the dimensions of the mirror are scaled down by a factor of 10. Inevitably, this gives rise to growing aberrations generated by the mirror. Hence, the subsequent imaging system requires a larger physical aperture, furthermore adding aberrations to the entire system. In contrast, due to the reduced feature sizes, the imaging system requires a smaller focal length compared to the previously discussed macroscopic setup. Considering all that, a redesign of the telecentric scanner for microscopic applications was performed [11]. The microscopic design has the same illumination wavelength as the system before.

7 Conclusion and outlook

The concept of a telecentric line scanning system with a torus mirror is a good approach to fulfill all conditions for a good telecentric image with a large field of view. This system is designed and developed to be a low-cost system, which is easy to handle and has a good flexibility to its fields of application. The system has good lateral and axial resolutions with low optical aberrations (point and field aberrations) in the whole system. The main application for that system is the inline processing, and it offers many advantages over ‘classical’ telecentric systems. However, given by the modular principle of the system, the use of several scanners in an alternating arrangement is also possible for the enlargement of the scan line. To additionally enhance the suitability of the telecentric line scanning system by providing even more flexibility to the setup, an incident light illumination can be realized by a coaxial setup [12], combining the illumination with the imaging setup. For this purpose, a beam splitter is placed between the imaging system and the detector.

To fit the illumination path to the geometry of the setup, this element requires a conic cross section (the shape of the beam-splitting surface) to successfully deflect the illuminating light onto the object. This setup creates other opportunities for industrial applications.

References

[1] R. W. Kessler, Prozessanalytik – Strategien und Fallbeispiele aus der industriellen Praxis (WILEY-VCH Verlag GmbH & Co KGaA, Weinheim, 2006).

[2] G. Schröder and H. Treiber, Technische Optik – Grundlagen und Anwendungen, 10., erweiterte Auflage (Vogel Buchverlag, Würzburg, 2007).

[3] R. Schuhmann and T. Thöniß, Telezentrishe Systeme für die optische Meß- und Prüftechnik (Technisches Messen 65(4), R. Oldenbourg Verlag, München, 1998).

[4] K. Donner, Vorrichtung zur optischen Erfassung von Prüfobjekten, EP2500716A2, Europäische Patentanmeldung (alfavision GmbH & Co. KG, Hutthurm, 2012).

[5] F. Loosen, W. Iff, N. Lindlein and K. Donner, Telezentrischer Linienscanner auf Basis eines Ringflächenspiegels zur Oberflächenanalyse von Bauteilen (Proceeding – 115. DGaO-Jahrestagung, Karlsruhe, 2014).

[6] F. Pedrotti, L. Pedrotti, W. Bausch and H. Schmidt, Optik für Ingenieure – Grundlagen (Springer-Verlag GmbH, Berlin, Heidelberg, 2005).

[7] L. Papula, Mathematik für Ingenieure und Naturwissenschaftler – Band 1, 12., überarbeitete und erweiterte Auflage (Vieweg+Teubner, GWV Fachverlage GmbH, Wiesbaden, 2009).

[8] R. Kingslake and R. Barry Johnson, Lens Design Fundamentals (Academic Press, Burlington, 2010).

[9] G. Litfin, Technische Optik in der Praxis, 3., aktualisierte und erweiterte Auflage (Springer-Verlag GmbH, Berlin, Heidelberg, 2005).

[10] A. W. Tronnier, Photographic objective comprising four lens members separated by air spaces and enclosing the diaphragm, US2673491A, Amerikanische Patentanmeldung (Voigtländer AG, Braunschweig, 1954).

[11] F. Loosen, N. Lindlein and K. Donner, A telecentric line scanning system: requirements in the macroscopic and microscopic regime (Proceeding – 116. DGaO-Jahrestagung, Brünn, 2015).

[12] STEMMER IMAGING, Das Handbuch der Bildverarbeitung (STEMMER IMAGING GmbH, 2013).

Florian Loosen
Institute of Optics, Information and Photonics, Friedrich-Alexander-Universität Erlangen-Nürnberg (FAU), Staudtstraße 7/B2 91058 Erlangen, Germany
florian.loosen@fau.de

Florian Loosen received his master's degree in 'Applied Physics' and his bachelor's degree in 'Optics and Laser Technology' at the RheinAhrCampus Remagen (Hochschule Koblenz – University of Applied Sciences). He continued his research as a PhD student in the research department of Prof. G. Leuchs at the Institute of Optics, Information and Photonics (research group of Prof. N. Lindlein) at the Friedrich-Alexander-Universität Erlangen-Nürnberg (FAU) until now. The topics of his theses (bachelor and master) were laser beam welding with a special design of a laser head and diffractive optical elements (DOEs) for polymer welding processes.

Norbert Lindlein
Institute of Optics, Information and Photonics, Friedrich-Alexander-Universität Erlangen-Nürnberg (FAU), Staudtstraße 7/B2 91058 Erlangen, Germany

Norbert Lindlein received his diploma in 'Physics' and his PhD at the Friedrich-Alexander-Universität Erlangen-Nürnberg (FAU). In 2002, he received his habilitation. After that, he was appointed as 'Privatdozent' and a few years later as 'Außerplanmäßiger Professor'. Currently, he is the group leader at the research group ODEM (Optical Design, Measurement and Microoptics) at the Institute of Optics, Information and Photonics of Prof. G. Leuchs. His research interests include the simulation and design of optical systems, diffractive optics, microoptics, and optical measurement techniques using interferometry or Shack-Hartmann wavefront sensors.

Klaus Donner
alfavision GmbH & Co. KG, Freyunger Straße 4, 94116 Hutthurm, Germany

Klaus Donner received his diploma in 'Mathematics' and his PhD at the Friedrich-Alexander-Universität Erlangen-Nürnberg (FAU) with emphasis on functional analysis and numerical mathematics. In 1981, he received his habilitation. After an associate professorship at the Universität der Bundeswehr München, he built up the educational branch of numerical and classical analysis from the corresponding chair at the University of Passau. Since his emeritation in 2010, he is the leading director of the R&D section of the alfavision GmbH & Co. KG, a spin-off enterprise in optical metrology and control systems.